

Hydrothermal Hexagonal $\text{SrFe}_{12}\text{O}_{19}$ Ferrite Powders: Phase Composition, Microstructure and Acid Washing

Ailin Xia,^{1,*} Xuzhao Hu,¹ Diankai Li,¹ Lu Chen,¹ Chuangui Jin,¹ Conghua Zuo,¹ and Shubing Su²

¹Anhui Key Laboratory of Metal Materials and Processing, School of Materials Science and Engineering, Anhui University of Technology, Maanshan 243002, China

²School of Electronic and Information Engineering, Ningbo University of Technology, Ningbo 315016, China

(received date: 2 April 2013 / accepted date: 19 July 2013 / published date: 10 March 2014)

A series of hexagonal *m*-type $\text{SrFe}_{12}\text{O}_{19}$ ferrite powders were hydrothermally synthesized, and their phase composition, microstructure and magnetic properties before/after acid washing were studied. In the synthesis of these specimens, the atomic ratio of Fe/Sr ($R_{\text{Fe/S}}$) in starting materials was set to 4, 5 and 12, respectively. When $R_{\text{Fe/S}} = 12$, the specimen has morphology of round flat cakes, not typical hexagonal plate-like structure. The results of SEM images and XRD patterns indicate that the specimen with $R_{\text{Fe/S}} = 12$ was mostly composed of Fe_2O_3 . When $R_{\text{Fe/S}} = 4$ or 5, the hexagonal plate-like $\text{SrFe}_{12}\text{O}_{19}$ ferrite powders were successfully synthesized with only a small quantity of Fe_2O_3 and SrCO_3 impurities. It is also found that acid washing can eliminate the impurities in as-synthesized specimens effectively, and also change their topography, which enhances the saturation magnetization. However, the coercivity changed irregularly after acid washing, which is ascribed to the combination of the changed morphology, introduced stress and lattice defects.

Keywords: $\text{SrFe}_{12}\text{O}_{19}$ ferrite, hydrothermal synthesis, acid washing, microstructure, magnetic properties

1. INTRODUCTION

As one of widely-used permanent magnetic materials, hexagonal *m*-type $\text{SrFe}_{12}\text{O}_{19}$ (SrM) ferrite is still attractive for its good combination of magnetic properties, performance-to-cost ratio and chemical stability.^[1-6] As a conventional chemical method, hydrothermal method has been used to synthesize SrM ferrite.^[1,7-9] Recently, we have synthesized a series of SrM ferrites via hydrothermal method,^[1] and found that it is very difficult to avoid the generation of SrCO_3 in the specimens since $\text{Sr}(\text{OH})_2$ is reactive with CO_2 in air, while the coprecipitation process and hydrothermal reaction did not occur in vacuum. Therefore, the atomic ratio of Fe/Sr ($R_{\text{Fe/S}}$) in starting materials should be set to lower than 12 due to the significant loss of Sr^{2+} ions during synthesis.^[7-9] However, when $R_{\text{Fe/S}} = 12$, what would happen to the specimen has not been reported. In addition, impurity Fe_2O_3 was also found as well as SrCO_3 in some specimens.^[1] These impurities have been believed to affect the magnetic properties of specimens. After our careful analysis, acid washing was identified as an effective way to eliminate these impurities. In this study, specimens of hexagonal SrM ferrite powders were hydrothermally synthesized with $R_{\text{Fe/S}} = 4$, 5 and 12, respectively, and the phase composition, microstructure and magnetic properties before/after acid washing were studied.

2. EXPERIMENTAL PROCEDURE

In this study, analytical class reagents were used for hydrothermal synthesis of SrM ferrite powders. The powder specimens were prepared by the following steps. First, aqueous solutions of $\text{Fe}(\text{NO}_3)_3$ and $\text{Sr}(\text{NO}_3)_2$ were coprecipitated by NaOH. According to the previous study,^[1] the molar ratio of $\text{OH}^-/\text{NO}_3^-$ ($R_{\text{OH/NO}_3^-}$) was set to 3, and the atomic ratio of Fe/Sr ($R_{\text{Fe/S}}$) was set to 4, 5 and 12, respectively. Secondly, the precipitates and aqueous solution were heated and underwent hydrothermal reaction in a Teflon liner at 220°C for 5 h. Finally, each of the obtained powders was divided into two parts. One part was washed only by deionized water, while the other part was washed by diluted hydrochloric acid (22 wt. %) and deionized water. For convenience, the specimens with $R_{\text{Fe/S}} = 4$, 5 and 12 are denoted as S₄, S₅ and S₁₂, respectively.

The phase composition of powder specimens was determined with a Rigaku D/max-2550V/PC x-ray diffractometer (XRD) using $\text{Cu K}\alpha$ radiation (wavelength $\lambda = 1.5418 \text{ \AA}$). The magnetic hysteresis loops were measured on an ADE EV-11 vibrating sample magnetometer (VSM) with a maximum external field $H_m \approx 1270 \text{ kA}\cdot\text{m}^{-1}$ ($\sim 16000 \text{ Oe}$). The micrographs were obtained on a JEOL JSM-6490LV scanning electron microscopy (SEM).

*Corresponding author: alxia@126.com
©KIM and Springer

3. RESULTS AND DISCUSSION

Figure 1(a) shows the XRD pattern of as-synthesized powder specimen S₁₂. Except for some unknown peaks, the figure only reveals the typical information of Fe₂O₃, while nearly no peak of hexagonal SrM ferrite is found. Therefore, SrM ferrite cannot be successfully synthesized under $R_{F/S} = 12$. It is thus clear that the ratio $R_{F/S} = 12$ is not suitable to hydrothermally synthesize SrM ferrite. Figure 1(b) is the typical SEM image of as-synthesized powder specimen S₁₂, and Fig. 1(c) is a typical SEM image of essentially pure SrM ferrite synthesized via hydrothermal method. In Fig. 1(b),

the powder specimen mostly composed of Fe₂O₃ has morphology of round flat cakes, while pure SrM ferrite powder has a hexagonal plate-like structure as shown in Fig. 1(c).^[1] It is well known that the morphology of Fe₂O₃ can be controlled in many ways.^[10-12] According to our experimental results to be published, if using nitrates as starting materials in hydrothermal reaction, the Fe₂O₃ obtained will have a round flat structure, which just resembles the morphology in Fig. 1(b). Obviously, the comparative study of SEM images in Fig. 1(b) and (c) confirms that hexagonal SrM ferrite can not be hydrothermally synthesized under $R_{F/S} = 12$.

Figure 2(a) and (b) show the XRD patterns of as-

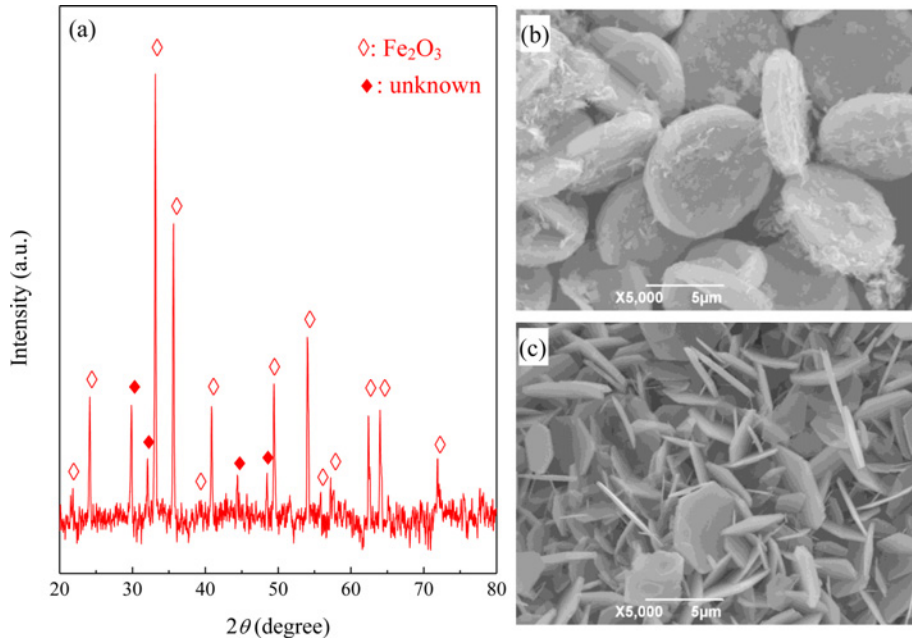


Fig. 1. XRD pattern (a) and typical SEM image (b) of as-synthesized SrM ferrite powder specimen with $R_{F/S} = 12$. (c): typical SEM image of essentially pure SrM ferrite powder synthesized via hydrothermal method.

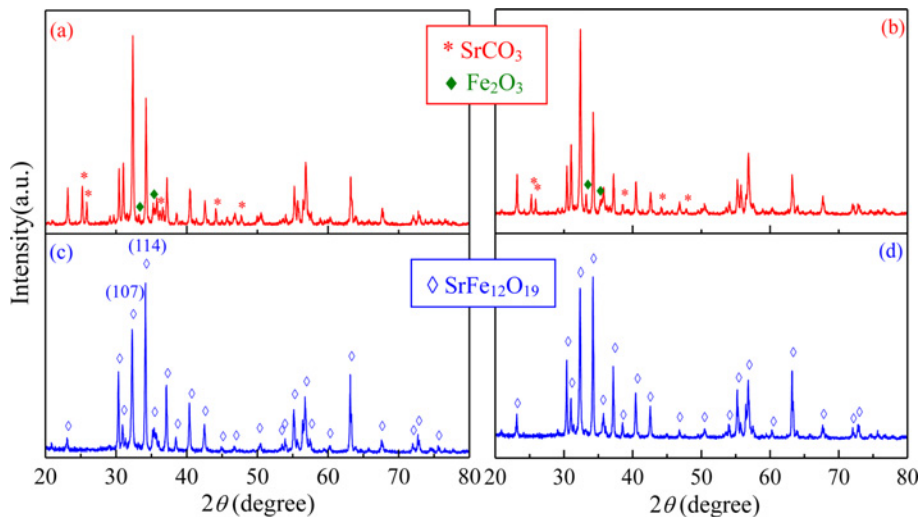


Fig. 2. XRD patterns of SrM ferrite powders before (a&b) / after (c&d) acid washing. (a&c): $R_{F/S} = 4$, (b&d): $R_{F/S} = 5$.

Table 1. Main magnetic properties, relative intensity of two strongest peaks ($I_{(107)}/I_{(114)}$) in XRD patterns, α , and average crystallite size, D , of synthesized SrM ferrite powders before/after acid washing.

	R_{FS}	M_s (emu/g)	H_c (kA/m)	α	D (nm)
before	4	54.7	40.2	1.48	62.6
	5	54.2	39.3	2.25	65.5
after	4	57.4	29.9	0.71	59.5
	5	61.4	60.4	0.92	68.3

synthesized powder specimens S_4 and S_5 . Both the patterns reveal the typical information of hexagonal SrM ferrite, which indicates that hexagonal $\text{SrFe}_{12}\text{O}_{19}$ phase has been synthesized successfully via hydrothermal method. However, also found are some impurity peaks from SrCO_3 and Fe_2O_3 in Fig. 2(a) and (b). It has been known that washing by diluted hydrochloric acid can eliminate impurity SrCO_3 and Fe_2O_3 . The XRD patterns of powder specimens S_4 and S_5 after acid washing are given in Fig. 2(c) and (d), respectively. Compared Fig. 2(a) to (c), (b) to (d), it is clear that all the impurity peaks vanish after acid washing, which means a pure hexagonal structure was obtained in specimens.

If we define the relative intensity of a peak (hkl) in Fig. 2 as $I_{(hkl)}$, the ratio of $I_{(hkl)}$ for two strongest peaks, $I_{(107)}/I_{(114)}$, can be defined as α . The values of α calculated from Fig. 2 are listed in Table 1. It is found that α decreases markedly after acid washing, which means more (114) crystalline planes were exposed to the air than (107) planes. Therefore, it can be deduced that the morphology of powder specimens

may be affected markedly by acid washing. Figure 3 shows the typical SEM micrographs of corresponding specimens. There are a lot of hexagonal plate-like structures in Fig. 3(a) and (b) which present the typical topography of as-synthesized SrM ferrite specimens before acid washing. The morphology is similar to the results of hydrothermally synthesized SrM ferrite powders in previous reports.^[7,9,13] It is thus clear that the results of SEM confirm the formation of hexagonal SrM ferrites. However, as shown in Fig. 3(c) and (d), after acid washing, many plates were broken into smaller irregular fragments, though there are still many unbroken hexagonal plate-like structures. Together with the change of α , it is clear that acid washing affects the topography and results in the exposure of more (114) crystalline planes in SrM ferrite powder specimens.

As is sensitive to the phase composition and topography of specimens, magnetic properties are sure to be affected by acid washing. Figure 4 gives the magnetic hysteresis loops of typical specimens S_5 before/after acid washing, and the saturation magnetization (M_s) and coercivity (H_c) of specimens S_4 and S_5 before/after acid washing are listed in Table 1. Acid washing eliminated the impurity SrCO_3 and Fe_2O_3 , which improves M_s in specimens. As seen from Table 1, for both S_4 and S_5 , the M_s increases to a certain degree after acid washing. However, the H_c decreases obviously for S_4 , while it increases markedly for S_5 , which exhibits an opposite tendency. As is known, the H_c obtained by VSM is not an intrinsic magnetic parameter, and is decided not only by chemical composition and crystalline structure, but also by

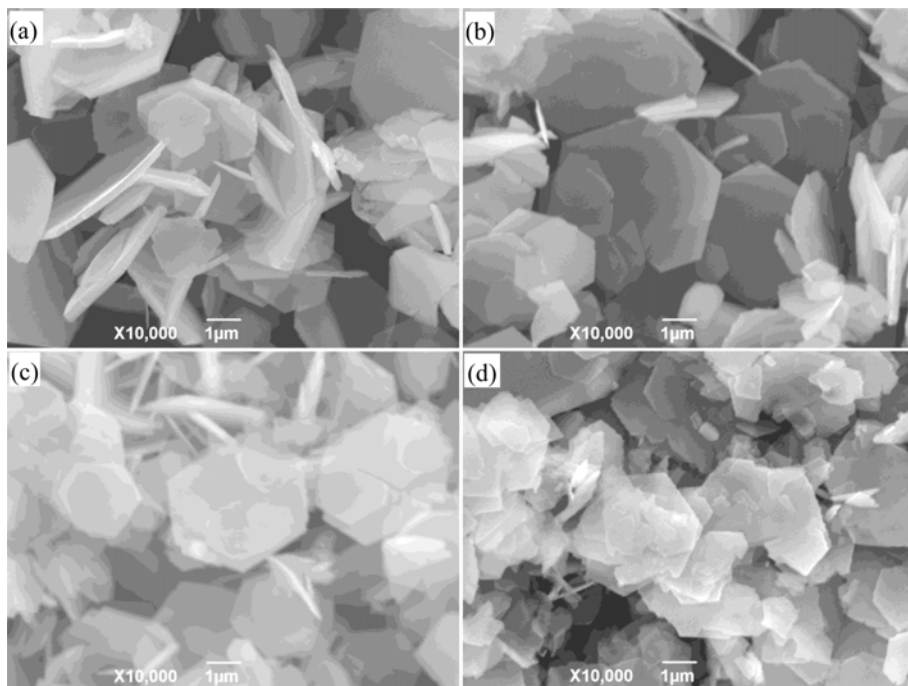


Fig. 3. Typical SEM images of SrM ferrite powders before (a&b) / after (c&d) acid washing. (a&c): $R_{FS} = 4$, (b&d): $R_{FS} = 5$.

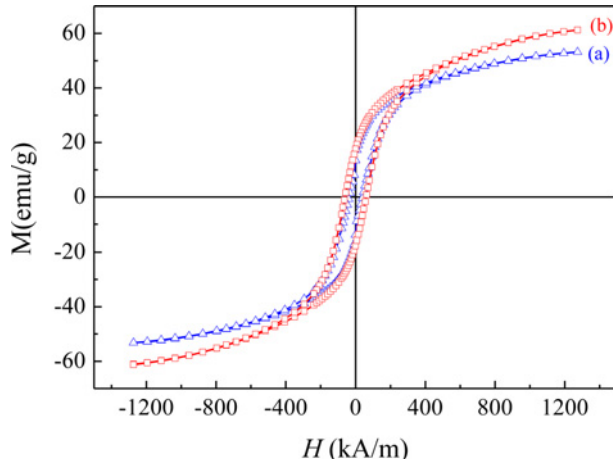


Fig. 4. Magnetic hysteresis loops of typical SrM ferrite powders before (a) / after (b) acid washing. $R_{F/S} = 5$.

average crystallite size (D), morphology, stress, lattice defects and so on. In our case, the values of D listed in Table 1 were calculated using Scherrer's equation. Clearly, though some grains were broken into smaller fragments, the average crystallite size, D , almost keeps unchanged after acid washing taking the calculation errors into accounting. Generally, D is thought to be the dominant factor that affects coercivity.^[14,15] As is discussed above, acid washing results in the exposure of more (114) crystalline planes in SrM ferrite powder specimens, which introduces more stress and lattice defects. Therefore, it is the combination of the changed morphology, introduced stress and lattice defects after acid washing that accounts for the conflicting change in the specimen S₄ and S₅.

4. CONCLUSIONS

In this study, hexagonal m -type $\text{SrFe}_{12}\text{O}_{19}$ (SrM) ferrite powder specimens were hydrothermally synthesized with various atomic ratio of Fe/Sr ($R_{F/S}$) in starting materials. The results of SEM images and XRD analysis of the specimens show that hexagonal SrM ferrites were successfully synthesized with $R_{F/S} = 4$ or 5, except $R_{F/S} = 12$. It has been found that acid washing can eliminate the impurities in as-synthesized specimens effectively, and also can change their topography,

which enhances the saturation magnetization, while affects the coercivity irregularly due to the combination of the changed morphology, introduced stress and lattice defects after acid washing.

ACKNOWLEDGEMENTS

This work was supported by the National Natural Science Foundation of China under Grant Nos. 11204003, 21071003 and the Natural Science Foundation of Ningbo under Grant No.2011A610182.

REFERENCES

1. A. L. Xia, C. H. Zuo, L. Chen, C. G. Jin, and Y. H. Lv, *J. Magn. Magn. Mater.* **332**, 186 (2013).
2. I. Ali, M. U. Islam, M. S. Awan, M. Ahmad, M. N. Ashiq, and S. Naseem, *J. Alloy. Compd.* **550**, 564 (2013).
3. M. A. Radmanesh and S. A. S. Ebrahimi, *J. Magn. Magn. Mater.* **324**, 3094 (2012).
4. M. Asghari, A. Ghasemi, and E. Paimozed, *Curr. Nanosci.* **8**, 239 (2012).
5. X. S. Liu, L. Fernandez-Garcia, F. Hu, and D. R. Zhu, *Mater. Chem. Phys.* **133**, 961 (2012).
6. D. Seifert, J. Töpfer, M. Stadelbauer, R. Grössinger, and J. L. Breton, *J. Am. Ceram. Soc.* **94**, 2109 (2011).
7. J. F. Wang, C. B. Ponton, and I. R. Harris, *J. Magn. Magn. Mater.* **234**, 233 (2001).
8. J. H. Lee, H. S. Kim, and C. W. Won, *J. Mater. Sci. Lett.* **15**, 295 (1996).
9. A. Ataie, I. R. Harris, and C. B. Ponton, *J. Mater. Sci.* **30**, 1429 (1995).
10. M. Žic, M. Ristić, and S. Musić, *J. Mol. Struct.* **993**, 115 (2011).
11. Y. Y. Xu, S. Yang, G. Y. Zhang, Y. Q. Sun, D. Z. Gao, and Y. X. Sun, *Mater. Lett.* **65**, 1911 (2011).
12. T. Sugimoto and Y. S. Wang, *J. Colloid Interface Sci.* **207**, 137 (1998).
13. J. F. Wang, C. B. Ponton, and I. R. Harris, *J. Alloy. Compd.* **403**, 104 (2005).
14. G. Herzer, *IEEE Trans. Magn.* **26**, 1397 (1990).
15. D. S. Xue, G. Z. Chai, X. L. Li, and X. L. Fan, *J. Magn. Magn. Mater.* **320**, 1541 (2008).